Organic & Biomolecular Chemistry

PAPER

View Article Online
View Journal | View Issue

Cite this: DOI: 10.1039/xxxxxxxxxx

Selective sensing of pyrophosphate in physiological media using zinc(II)dipicolylamino-functionalised peptides†

Vincent E. Zwicker, Benjamin M. Long and Katrina A. Jolliffe*

Received Date
Accepted Date

DOI: 10.1039/xxxxxxxxxx

www.rsc.org/journalname

A series of linear peptide based anion receptors, in which the distance between the bis[zinc(II)dipicolylamine] binding sites and the peptide backbone was varied systematically, was prepared and their anion binding ability was investigated using indicator displacement assays. Shortening the distance between the binding site and the peptide backbone was found to enhance both the receptor affinity and selectivity for pyrophosphate over other organic polyphosphate anions in Krebs buffer with the maximum selectivity and affinity observed with a spacer length of two methylene units. The suitability of these receptors for the determination of pyrophosphate concentrations in Krebs buffer and in artificial urine was examined.

Introduction

Anions play a major role in a variety of chemical and biological processes and the selective recognition of anionic species has become an important research area.[1–5] The pyrophosphate (PPi) anion is involved in a number of biochemical reactions and thus, the determination of its concentration in physiological environments has applications in the diagnosis and monitoring of several diseases.[6–9] However, discrimination between PPi and other biologically relevant phosphate oxoanions such as adenosine di- and triphosphate (ADP and ATP) remains a significant challenge.[10–14]

Bis zinc(II)dipicolylamine complexes have been found to exhibit remarkable selectivity for phosphates over other anions in aqueous media.[15] Recently, we have shown that linear tri- and tetra-peptide based receptors bearing two zinc(II)-dipicolylamine (Zn(II)-DPA) functionalised lysine (Lys) side chains exhibit considerable selectivity for PPi over ADP and ATP in HEPES buffer and we illustrated that the PPi binding capability of these receptors was dependent on the nature of the non-functionalised side chains.[16] We envisaged that affinity and selectivity for PPi over ADP and ATP might also be altered by varying the length of the functionalised Lys side chains, as has previously been observed for cyclic peptide-based anion receptors.[17,18]

Herein, we demonstrate – using indicator displacement assays (IDAs) – that installing the Zn(II)-DPA units in closer proximity to the peptide backbone enhances receptor affinity and selectivity for PPi over ADP and ATP in Krebs buffer. We subsequently demonstrate the suitability of our chemosensors for the quantification of PPi in Krebs buffer and in artificial urine. The latter medium was chosen as it has been suggested that the PPi content in human urine is related to the formation of renal calculi and consequently, the determination of PPi in urine would allow the diagnosis or monitoring of kidney related diseases.[9] To investigate the effect of distance between the Zn(II)-DPA units and the peptide backbone on anion binding, we chose to systematically reduce the length of the amino acid side chains from four to one methylene units to give receptors **1**-**4**·$\mathbf{Zn_2}$ (Fig. 1). We also prepared receptor **5**·$\mathbf{Zn_2}$ in which the two Zn(II)-DPA units were attached to side chains of different length to see how this influenced anion binding.

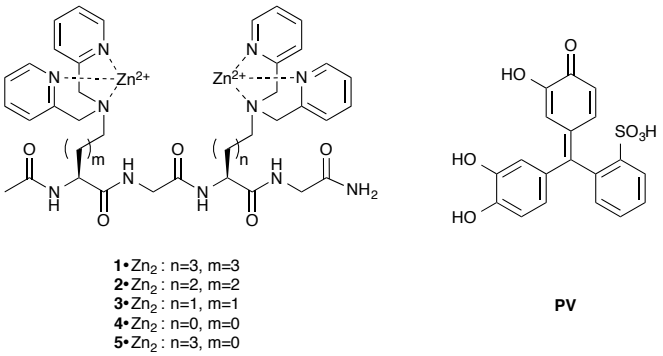

Fig. 1 Structures of receptors **1**-**5**·$\mathbf{Zn_2}$ and indicator **PV**.

† Electronic Supplementary Information (ESI) available: NMR and mass spectra for all new compounds and anion titration data including buffer compositons. See DOI: 10.1039/b000000x/

* *School of Chemistry, The University of Sydney, 2006, NSW, Australia. E-mail: kate.jolliffe@sydney.edu.au; Tel: +61 2 9351 2297*

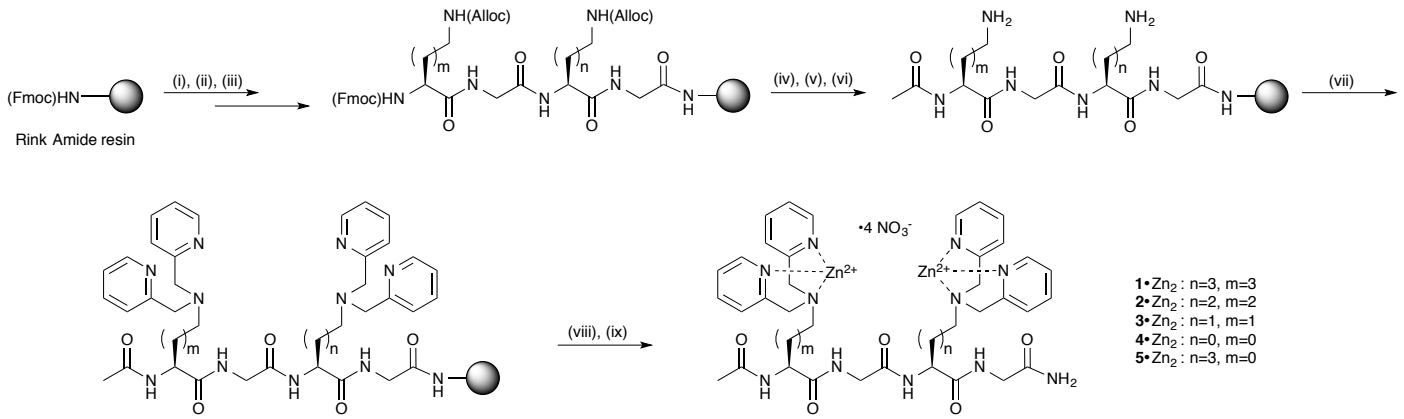

Scheme 1 Synthetic route for the preparation of receptors **1-5·Zn$_2$**. Conditions: (i) Fmoc deprotection of Rink Amide resin: 20 vol% piperidine in DMF; (ii) Loading: Fmoc-Gly-OH (3 equiv.), PyBOP (3 equiv.) and DIPEA (6 equiv.); (iii) Iterative Fmoc-SPPS: (a) Fmoc deprotection: 20 vol% piperidine in DMF; (b) coupling: Fmoc-AA-OH (2.5-3 equiv.), PyBOP (2.5-3 equiv.), DIPEA (5-6 equiv.), DMF; (iv) N-terminal Fmoc deprotection: 20 vol% piperidine in DMF; (v) Acetylation: 20 vol% acetic anhydride in pyridine; (vi) Alloc deprotection: $Pd(PPh_3)_4$ (0.8 equiv.), $PhSiH_3$ (25 equiv.), CH_2Cl_2; (vii) Reductive amination: (a) 2-pyridinecarboxaldehyde (20 equiv.), 1 vol% acetic acid, DMF; (b) 2-pyridinecarboxaldehyde (20 equiv.), sodium triacetoxyborohydride (25 equiv.), 1 vol% acetic acid, DMF; (viii) Cleavage: TFA/TIS/H_2O (95:2.5:2.5, v/v/v); (ix) Complexation: $Zn(NO_3)_2$ (2 equiv.), MeOH/H_2O (1:1, v/v).

Results and discussion

Synthesis of Receptors 1-5·Zn$_2$

Receptors **1-5·Zn$_2$** were synthesised using our previously reported synthetic route,[16] with slight modifications. Briefly, the linear peptides were synthesised using Fmoc solid phase peptide synthesis (Fmoc-SPPS) on Rink amide resin, employing the amino acid L-lysine (L-Lys) or its shorter analogues L-ornithine (L-Orn), L-2,4-diaminobutyric acid (L-Dab), and L-2,3-diaminopropionic acid (L-Dap), all with appropriate side chain protection, in the coupling steps. Subsequent acetylation of the N-terminal amine and deprotection of the amino side chain groups were followed by on-resin reductive amination to install the DPA ligands. A glycine (Gly) spacer was incorporated at the C-terminus of all peptides as we have previously found that this facilitiates the on-resin reductive amination reaction.[16] Cleavage from the resin and purification gave the DPA functionalised peptides **1-5** in 22-26% yields (based on a resin loading of 0.55 mmol g^{-1}), and quantitative complexation with two equiv. of zinc nitrate afforded receptors **1-5·Zn$_2$** as nitrate salts (Scheme 1).

Anion binding studies

Anion binding studies were performed in Krebs buffer using IDAs[19] with the previously employed colorimetric indicator pyrocatechol violet **PV**.[16,17,20–22] We first investigated the interaction between **PV** and receptors **1-5·Zn$_2$**. Equimolar solutions of **PV** (20 μM) and receptors **1-5·Zn$_2$** (20 μM) in Krebs buffer displayed a distinctive blue colour. Association constants (log K_a) for the respective indicator-receptor complexes (Table 1) were determined by UV-Vis titrations of **PV** (20 μM) with receptors **1-5·Zn$_2$** (Fig. 2 and Fig. S1-S5, †ESI) and non-linear least square fitting of the titration data to a 1:1 binding model using the commercially available program HypSpec® (Hyperquad® package).[23] The 1:1 binding stochiometry between receptors **1-5·Zn$_2$** and indicator **PV** was corroborated by Job's plot analysis (Fig. S13-S15, †ESI). Interestingly, the log K_a values for all

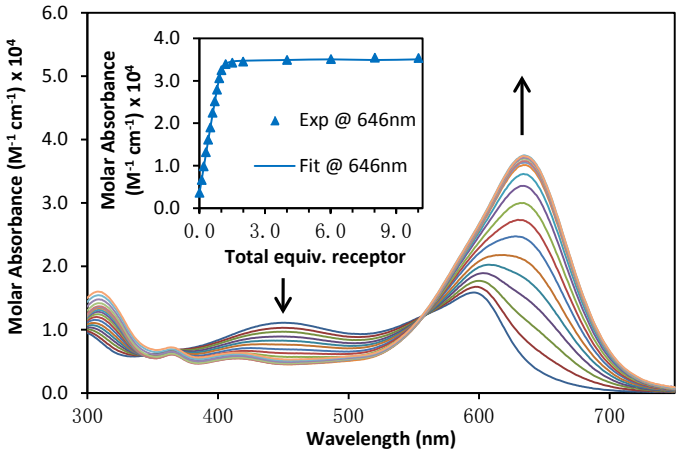

Fig. 2 Representative UV-Vis spectra showing the changes in molar absorbance of **PV** (20 μM) in Krebs buffer upon the addition of receptor **3·Zn$_2$**, [**3·Zn$_2$**]=0, 2, 4, 6, 8, 10, 12, 14, 16, 18, 20, 23, 29, 39, 74, 107 μM; inset: fitting curve for the titration data at 646 nm to a 1:1 binding model.

receptor-indicator pairs were similar (log K_a ranging from 6.8 to 6.9) except for receptor **4·Zn$_2$** which exhibited noticeably weaker binding to **PV** (log K_a=6.2). We reasoned that the lower binding affinity between **4·Zn$_2$** and **PV** is a result of steric hindrance resulting from the short distance between the Zn(II)-DPA binding sites and the peptide backbone.

Subsequently, 1:1–indicator:receptor mixtures (20 μM each) were prepared and 10 equiv. of a wide range of anions were added. For all **PV**–receptor mixtures, the addition of PPi resulted in a colour change from blue to yellow, indicating the displacement of **PV** from the binding cavity. The addition of ATP or ADP gave only small colour changes and the addition of all other anions tested did not result in a naked-eye observable colour change, indicating only partial or no indicator displacement, respectively (Fig. 3). UV-Vis titrations of 1:1–indicator:receptor mix-

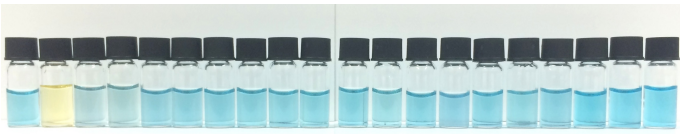

Fig. 3 Colour changes of a solution of **3·Zn$_2$** : **PV** (20 μM each) upon the addition of 10 equiv. of various anions. From left to right: blank, PPi, ATP, ADP, AMP, cAMP, TMP, p-Ser, p-Thr, p-Tyr, citrate, sodium ascorbate, Na_2CO_3, $Na_2S_2O_3$, KSCN, $NaNO_2$, Na_2SO_4, Na_3PO_4, NaBr, NaI.

Table 1 Association constants (log K_a) for receptors **1**-**5**·**Zn$_2$** and indicator **PV**, PPi, ATP, and ADP [a]

Receptor	Indicator **PV**	PPi	ATP	ADP
1·Zn$_2$	6.9	7.0	4.5	4.0
2·Zn$_2$	6.8	7.3	4.0	3.9
3·Zn$_2$	6.8	7.5	4.1	4.0
4·Zn$_2$	6.2	5.0	3.8	3.9
5·Zn$_2$	6.8	5.9	4.1	4.1

[a] Titrations were performed at 25 °C in Krebs buffer, pH 7.4; estimated error in log $K_a < 0.2$

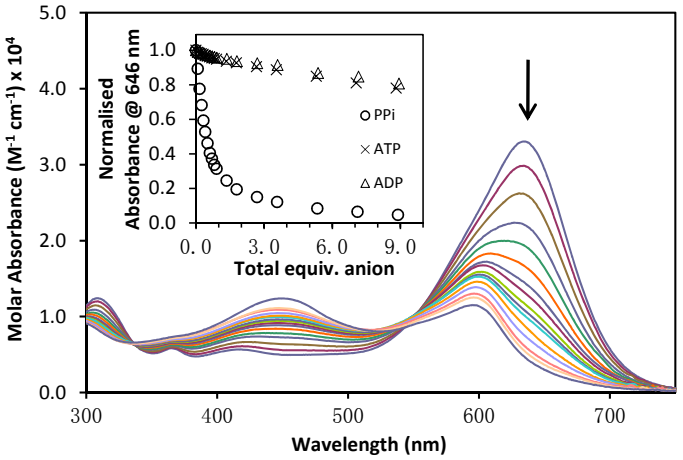

Fig. 4 Representative UV-Vis spectra showing the changes in molar absorbance of a 1:1–**PV**:**3·Zn$_2$** mixture (20 μM each) in Krebs buffer upon the addition of PPi, [PPi]=0, 2, 3, 5, 6, 8, 10, 12, 14, 16, 18, 26, 35, 52, 68, 101, 132, 162 μM; inset: changes in the normalised absorbance at 646 nm of this mixture upon addition of up to 9 equiv. of PPi, ATP or ADP, respectively.

tures with the sodium salts of PPi, ATP and ADP (Fig. 4 and Fig. S7-S9, †ESI) and curve-fitting of the titration data (based on the equilibria for competition assays[24]) using the HypSpec® program gave the association constants for the receptor:anion complexes (Table 1). In comparison to receptors **1**-**3**·**Zn$_2$**, receptor **4**·**Zn$_2$** exhibited weaker binding to PPi, attributable to the short distance between the Zn(II)-DPA units and the peptide backbone, which apparently hinders PPi from accessing the binding sites due to steric repulsion. Receptor **5**·**Zn$_2$** binds PPi less strongly than receptors **1**-**3**·**Zn$_2$** but more strongly than receptor **4**·**Zn$_2$**, demonstrating that the receptor affinity for PPi can be tuned by varying the distance between the Zn(II)-DPA binding sites and the peptide backbone. Receptor **1**·**Zn$_2$** exhibited strong binding to PPi and good selectivity for PPi over ATP and ADP. Compared to receptor **1**·**Zn$_2$**, receptors **2**·**Zn$_2$** and **3**·**Zn$_2$** exhibited stronger binding to PPi and enhanced selectivity for PPi over ATP and ADP.

We rationalised the stronger binding affinity of receptors **2**·**Zn$_2$** and **3**·**Zn$_2$** for PPi by postulating favourable secondary hydrogen bonding interactions between the N–H functionalities of the peptide backbone and the oxygen atoms of PPi, which would emerge as the Zn(II)-DPA binding sites are brought into closer proximity to the peptide backbone. Our hypothesis was supported by molecular modelling of the receptor **3**·**Zn$_2$**–PPi complex, suggesting the formation of three hydrogen bonds, *i.e.* between two of the PPi oxygen atoms and three of the NH protons; specifically the C-terminal NH_2 group, the N-terminal acetamide proton, and the proton of the next amide along the chain from the N-terminus (Fig. 5). Molecular modelling of the receptor **1**·**Zn$_2$**–PPi complex suggested that the distance between the Zn(II)-DPA bonded PPi anion and the peptide backbone is too far for hydrogen bonding interactions to occur (Fig. S16, †ESI).

^{1}H NMR experiments further supported our hypothesis that secondary interactions between the peptide backbone and PPi are responsible for the observed increase in PPi affinity of receptor **3**·**Zn$_2$** compared to receptor **1**·**Zn$_2$**. ^{1}H NMR titrations of receptors **1**·**Zn$_2$** and **3**·**Zn$_2$** with HPPi as the TBA salt were performed in DMSO-d_6 (in order to allow the NH proton signals to be observed) as we envisaged that the formation of hydrogen bonds between the involved NH groups and the PPi oxygen atoms would result in a change in the chemical shift δ of the respective NH signals. Interestingly, for receptor **3**·**Zn$_2$**, the addition of HPPi resulted in the formation of a sharp new signal at 6.91 ppm (Fig. S20), which was attributed to one of the two C-terminal carboxamide NH protons through a combination of 2D NMR and proton exchange experiments (Fig. S17-S22 and S25, †ESI). We concluded that the signal at 6.91 ppm emerges as a consequence of the induction of a conformational change upon binding of HPPi, thus indicating the formation of a hydrogen bond between one of the carboxamide NHs and HPPi. In contrast, the addition of HPPi to receptor **1**·**Zn$_2$** did not result in similar changes to the corresponding NH signal (Fig. S24, †ESI), confirming that the distance between the binding sites and the peptide backbone plays a crucial role for the occurrence of secondary interactions in our host–guest systems.

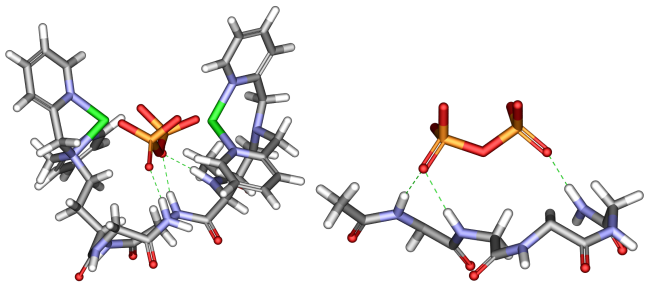

Fig. 5 DFT-optimised molecular structures of: (left) the **3**·**Zn$_2$**–PPi complex and (right) the **3**·**Zn$_2$**–PPi complex upon rotation about the *z*-axis where the Zn(II)-DPA side arms have been omitted for clarity; hydrogen bonds are represented by the green dashed lines.

In order to monitor the binding process of PPi to **3**·**Zn$_2$** we carried out ^{31}P-NMR studies, titrating a solution of PPi in D_2O with receptor **3**·**Zn$_2$** (Fig. S26, †ESI). The PPi signal at −9.3 ppm

moved gradually downfield with addition of **3·Zn$_2$** – indicating the interaction of **3·Zn$_2$** with PPi – and disappeared upon the addition of 1.1 equiv. of **3·Zn$_2$**. New signals at −8.3 ppm and at −5.0 ppm grew in after the addition of 0.1 equiv. and 0.5 equiv. of **3·Zn$_2$**, respectively. We assigned the signal at −5.0 ppm to the 1:1–PPi:**3·Zn$_2$** complex and rationalised that the signal at −8.3 ppm can be attributed to a 2:1–PPi:**3·Zn$_2$** complex which is thought to form in the presence of excess PPi. The signal at −8.3 ppm decreased and the signal at −5.0 ppm appeared upon the addition of 0.5 equiv. of **3·Zn$_2$**, suggesting that as more receptor is added, the 1:1–PPi:**3·Zn$_2$** complex is the dominant species in solution. Given the high affinity and excellent selectivity for PPi over ATP and ADP which we observed for the **3·Zn$_2$:PV** chemosensing ensemble, we investigated its suitability for use in biological PPi sensing applications *i.e.* for the determination of PPi in Krebs buffer and in artificial urine.[25] Firstly, the impact of biological relevant anions such as ATP, ADP, AMP, and others on the photometric response of the **3·Zn$_2$:PV** chemosensing ensemble to PPi in Krebs buffer was examined. Upon addition of 10.0 equiv. of the tested anions, the **3·Zn$_2$:PV** ensemble exhibited negligible changes in the ratiometric absorbance, $\Delta(A_{440\ nm}/A_{646\ nm})$, except in the case of ATP and to a slighter extent ADP, suggesting that most of the tested anionic species were not able to displace **PV** from the **3·Zn$_2$:PV** complex (Fig. 6). Subsequent addition of PPi (1.0 equiv.) resulted in significant changes in the ratiometric absorbance in all cases, indicating successful indicator displacement and demonstrating the capability of **3·Zn$_2$** to selectively bind PPi even in the presence of a large excess of other phosphoanions. [PPi] calibrations were carried out in Krebs buffer without and with 200 μM ATP, as our results above showed that ATP interfered most strongly with the response of **3·Zn$_2$:PV** to PPi. Gratifyingly, steady absorbance changes of the **3·Zn$_2$:PV** chemosensing ensemble were observed upon the addition of PPi in both the absence and presence of ATP and linear calibration curves were obtained over a [PPi] range from 2 to 38 μM in both cases (Fig. S27, †ESI and Fig. 7, respectively). These results suggest that the presence of ATP does not have a significant impact on the capability of **3·Zn$_2$:PV** to detect PPi and that PPi concentrations of down to 2 μM ($3{\cdot}s_{y/x}$/slope) can be detected in both cases (see Fig. S27-28, †ESI for a detailed outline of the statistical treatment of this data).

To further explore the suitability of the **3·Zn$_2$:PV** sensing system for biological applications, we carried out PPi binding studies in artificial urine. Despite the 40% higher ionic strength and the 20 times higher phosphate concentration of artificial urine[25] compared to that of Krebs buffer (†ESI), the **3·Zn$_2$:PV** chemosensing ensemble remained functional. UV-Vis titrations of **PV** (20 μM) with **3·Zn$_2$** indicated the formation of the expected 1:1–indicator:receptor complex (Fig. 8). Fitting of the titration data to a 1:1 binding model gave a log K_a of 5.6 ± 0.2 for the **3·Zn$_2$:PV** complex in this medium. Upon titration of **3·Zn$_2$:PV** with PPi and subsequent 1:1 curve fitting, a log K_a of 6.8 ± 0.2 for the **3·Zn$_2$**:PPi complex was obtained. Given the significantly higher concentration of solutes in artificial urine and thus, the considerably increased competitiveness of this medium compared to Krebs buffer, these results underline the excellent affinity and

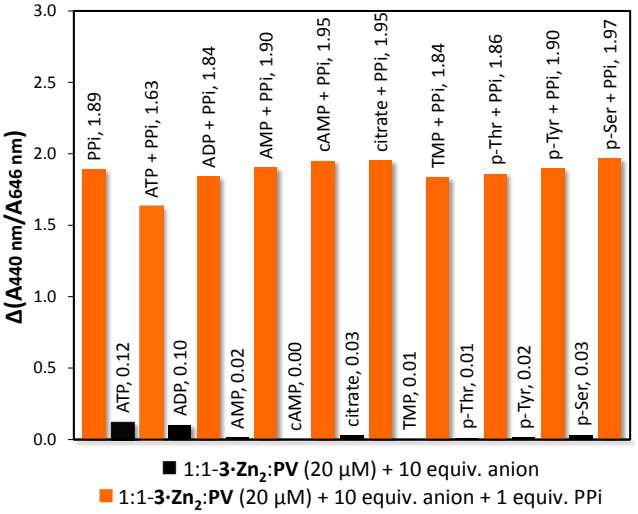

Fig. 6 Changes in ratiometric absorbance of a solution of **3·Zn$_2$** : **PV** (20 μM each) upon the addition of 10.0 equiv. of various anions (■) and upon the addition of 10.0 equiv. of various anions and 1.0 equiv. of PPi (■).

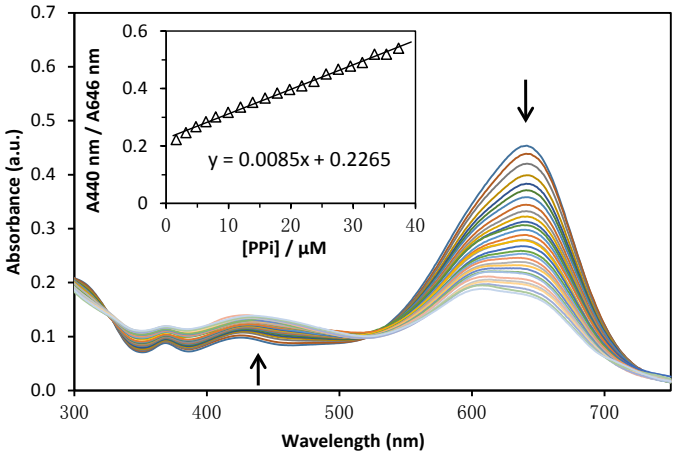

Fig. 7 UV-Vis spectrum showing the changes in absorbance of a solution of **3·Zn$_2$:PV** (20 μM each) in Krebs buffer (25 °C, pH 7.4) upon the addition of PPi (0.0–3.0 equiv.) in the presence of ATP (200 μM). Inset: Corresponding calibration plot for [PPi], $A_{440\ nm}/A_{646\ nm} = f([\mathrm{PPi}])$.

selectivity of the **3·Zn$_2$:PV** chemosensing ensemble for PPi. Subsequently, we carried out [PPi] calibration experiments with the **3·Zn$_2$:PV** system in artificial urine (Fig. 9) and obtained a linear calibration curve in the [PPi] range from 2 to 22 μM, indicating that PPi concentrations as low as 4 μM ($3{\cdot}s_{y/x}$/slope) can be detected in artificial urine.

Conclusions

In summary, the anion binding capability of a series of tetrapeptide based receptors was investigated. By systematically varying the distance between the two Zn(II)-DPA binding sites and the peptide backbone we have shown that, up to a point, decreasing this distance results in incremental increases on both PPi binding affinity and selectivity for this species over other phosphoanions. The optimum length for the DPA side chains was found to be

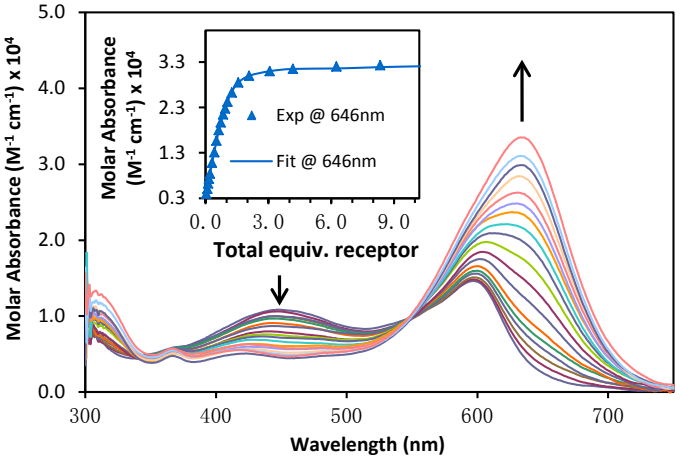

Fig. 8 UV-Vis spectrum showing the changes in molar absorbance of **PV** (20 μM) in artificial urine (25 °C, pH 7.4) upon the addition of receptor **3·Zn$_2$**, [**3·Zn$_2$**]=0, 1, 2, 3, 4, 6, 8, 10, 12, 14, 16, 18, 20, 24, 30, 40, 77, 112 μM; inset: fitting curve for the titration data at 646 nm to a 1:1 binding model.

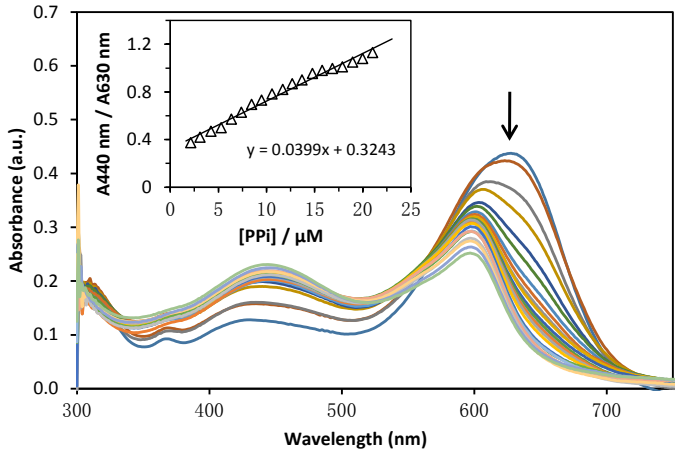

Fig. 9 UV-Vis spectrum showing the changes in absorbance of a solution of **3·Zn$_2$**:**PV** (20 μM each) in artificial urine (25 °C, pH 7.4) upon the addition of PPi (0.0–2.0 equiv.); Inset: Corresponding calibration plot for [PPi], $A_{440\ nm}/A_{630\ nm} = f([PPi])$.

two methylene units. Shortening the side chains further resulted in a decrease in both receptor affinity and selectivity. Using a combination of NMR and modelling studies we have shown that decreasing the distance between the Zn(II)-DPA binding sites and the peptide backbone is likely to provide additional hydrogen bonding interactions between the peptide backbone and the PPi oxygen atoms and thus, increases the receptor affinity for PPi. Finally, we demonstrated that these chemosensing ensembles are able to detect PPi in complex competitive media such as Krebs buffer – even in the presence of high concentrations of ATP and other phosphoanions – and in artificial urine. Current studies are underway to assess the suitability of our systems for the determination of PPi in clinical samples of human urine and synovial fluid.

Experimental section

General information

All chemicals and solvents were of reagent grade and used as received unless otherwise noted. Fmoc-Dab-OH, and Fmoc-Dap-OH were synthesised following slightly modified literature procedures[26] and Fmoc-Dab(Alloc)-OH, and Fmoc-Dap(Alloc)-OH were obtained by subsequent side chain protection with the (Allyloxy)carbonyl (Alloc) group.[27] Fmoc-Orn(Alloc)-OH was obtained by side chain deprotection of Fmoc-Orn(Boc)-OH and subsequent protection of the free amine functionality with the Alloc group.[27] Fmoc-Lys(Alloc)-OH was obtained commercially. Melting points were manually observed using a Stanford Research Systems Optimelt melting point apparatus and are uncorrected. Optical rotations were obtained using a Perkin Elmer Model 341 polarimeter at 589 nm and 20 °C, using the indicated spectroscopic grade solvents. ^{1}H NMR spectra were recorded using a Bruker Avance III 500 at a frequency of 500.13 MHz or a Bruker Avance DPX 400 at a frequency of 400.13 MHz and are reported as parts per million (ppm) with CD_3OD (δ_H 3.31 ppm) or DMSO-d_6 (δ_H 2.50 ppm) as an internal reference. The data are reported as chemical shift (δ), multiplicity (br = broad, s = singlet, d = doublet, t = triplet, m = multiplet), coupling constant (J Hz) and relative integral. ^{13}C NMR spectra were recorded using a Bruker Avance III 500 at a frequency of 125.76 MHz or a Bruker Avance DPX 400 at a frequency of 100.61 MHz and are reported as parts per million (ppm) with CD_3OD (δ_C 49.00 ppm) or DMSO-d_6 (δ_C 39.52 ppm) as an internal reference. ^{31}P{^{1}H} NMR spectra were recorded using a Bruker Avance III 500 at a frequency of 202.46 MHz and are reported as parts per million (ppm) relative to trimethyl phosphate, $(CH_3O)_3PO$, in D_2O (0 ppm). Low resolution mass spectra were recorded on a Thermo Finnigan LCQ Deca Ion Trap mass spectrometer using electrospray ionisation (ESI, positive mode). High resolution ESI spectra were recorded on a Bruker BioApex Fourier Transform Ion Cyclotron Resonance mass spectrometer (FTICR) with an Analytica ESI source, operating at 4.7 T or a Bruker Daltonics Apex Ultra FTICR with an Apollo Dual source, operating at 7 T and are reported as m/z (relative intensity). Infrared absorption spectra were recorded on a Bruker Alpha-E FT-IR spectrometer using attenuated total reflection (ATR) of either a solid or a thin film. Notable vibrational wavenumbers are recorded in cm^{-1}. UV-Vis data were recorded using a Varian Cary 4000 UV-Vis spectrophotometer at 20 °C. Temperature control was provided by a Varian Cary PCB 150 Water Peltier System. pH values were obtained using an Activon Model 209 pH/mV meter. Reversed-phase column chromatography was performed on a Biotage Isolera Prime automated flash purification system equipped with a dual wavelength UV-Vis detector. The detection wavelengths were 254 and 280 nm, respectively. Molecular structures were modelled employing molecular mechanic force field (MMFF) calculations and MMFF structures were fully optimised using DFT calculations at the B3LYP/6-31G* level of theory (Spartan'04).

General procedures for SPPS of receptors 1-5·Zn_2

Loading of Fmoc-protected amino acid onto Rink amide resin. Rink amide resin (loading 0.55 mmol g^{-1}) was swollen in DMF for 1 h. The resin was drained and washed with DMF (×5), CH_2Cl_2 (×5) and DMF (×5). The resin was then treated with 20 vol% piperidine in DMF (3 × 5 min) for Fmoc deprotection and washed with DMF (×5), CH_2Cl_2 (×5) and DMF (×5). A solution of Fmoc-Gly-OH (3 equiv.), PyBOP (benzotriazol-1-yl-oxytripyrrolidinophosphonium hexafluorophosphate; 3 equiv.), and DIPEA (*N,N*-diisopropylethylamine; 6 equiv.) in DMF was added to the resin. The suspension was agitated at rt for 2 h and then washed with DMF (×5), CH_2Cl_2 (×5) and DMF (×5).

N-terminal Fmoc deprotection. The resin-bound peptide was treated with 20 vol% piperidine in DMF (3 × 10 min) for Fmoc deprotection and washed with DMF (×5), CH_2Cl_2 (×5) and DMF (×5). The resulting free amine was immediately subjected to the following coupling step.

Estimation of resin loading. The drained Fmoc deprotection solution was diluted with a solution of 20 vol% piperidine in DMF so that the maximum concentration of the fulvene-piperidine adduct was in the range of 2.5-7.5×10^{-5} M. A sample of this solution (2 × 3 mL) was transferred to two matched 1 cm quartz glass cuvettes and the UV-Vis absorbance at 301 nm was measured, using the solution of 20 vol% piperidine in DMF as a reference. An average of the two absorbance values was used to calculate the loading, using $\varepsilon = 7800$ M^{-1} cm^{-1}.

Amino acid coupling. A solution of the respective amino acid (2.5-3 equiv.), PyBOP (2.5-3 equiv.), and DIPEA (5-6 equiv.) in DMF was added to the resin. The suspension was agitated at rt for 2 h and then washed with DMF (×5), CH_2Cl_2 (×5), and DMF (×5).

Acetylation. After coupling of the final amino acid, the Fmoc protecting group was removed. The free amine functionality was acetylated by treatment with 20 vol% acetic anhydride in pyridine (3 × 5 min) and washed with DMF (×5), CH_2Cl_2 (×5), and DMF (×5).

(Allyloxy)carbonyl (Alloc) deprotection. The resin was swollen in CH_2Cl_2 at rt for 1 h prior to the deprotection step. The resin was agitated in a solution of $Pd(PPh_3)_4$ (0.8 equiv.) and phenylsilane (25 equiv.) in CH_2Cl_2 (2 × 1 h). The resin was rinsed and washed with CH_2Cl_2 (×5), a solution of sodium diethyldithiocarbamate (20 mg mL^{-1}) with 1 vol% triethylamine in DMF (×10), DMF with 1 vol% triethylamine (×5), DMF (×5), and CH_2Cl_2 (×5) and dried *in vacuo* overnight.

Reductive amination. The resin was swollen in DMF at rt for 1 h before being treated with 2-pyridinecarboxaldehyde (20 equiv.) with 1 vol% AcOH in DMF (5 mL) and agitated at rt overnight. The resin was rinsed and washed with DMF (×3). A suspension of sodium triacetoxyborohydride (25 equiv.) and 2-pyridinecarboxaldehyde (20 equiv.) with 1 vol% AcOH in DMF (5 mL) was added to the resin and the resulting suspension was agitated at rt overnight. The resin was rinsed and washed with MeOH (3 × 5 mL), DMF (×5), CH_2Cl_2 (×5), and DMF (×5) and dried *in vacuo* overnight.

Cleavage of peptides from resin. The resin was treated with a solution of trifluoroacetic acid/H_2O/triisopropylsilane (95:2.5:2.5, v/v/v) for 1 h. The resin was drained and then washed with trifluoroacetic acid (×3). The cleavage solution and acid washes were combined and the solvent evaporated.

Purification. Peptides were purified by reversed-phase column chromatography (25 g C_8-reversed phase silica gel; water/CH_3CN with 1 vol% ammonium hydroxide solution (25%), 0 to 50% CH_3CN, 75 mL min^{-1}). Appropriate fractions were lyophilised, affording the pure peptides as colourless solids.

Complexation to zinc. A solution of peptide in MeOH (10 mg mL^{-1}) was added to an aqueous solution of $Zn(NO_3)_2 \cdot 4H_2O$ (2 equiv. relative to peptide, 10 mg mL^{-1}) and the mixture was stirred at rt for 1 h. The mixture was concentrated and the residue lyophilised, affording the bis[Zn(II)] complex as a nitrate salt.

Synthesis

Ac-Lys(DPA)-Gly-Lys(DPA)-Gly-NH_2 zinc complex, 1·Zn_2 Tetrapeptide **1** was synthesised on Rink amide resin (0.451 g, resin capacity 0.55 mmol g^{-1}), utilising the above general methods. Yield: 47.2 mg (25%); $[\alpha]_D^{20} = -22.9$ (*c* 0.60 MeOH); ^{1}H NMR (500 MHz, MeOD) δ 8.42 (m, 4H), 7.79 (m, 4H), 7.61 (m, 4H), 7.26 (m, 4H), 4.20 (m, 1H), 4.13 (m, 1H), 3.76-3.93 (m, 12 H), 2.51 (m, 4H), 1.93 (s, 3H), 1.55-1.80 (m, 8H), 1.33 (m, 4H), NH signals not observed; ^{13}C NMR (75 MHz, MeOD) δ 175.4, 174.7, 174.3, 173.7, 172.1, 160.83, 160.80, 149.4, 149.3, 138.69, 138.65, 124.86, 124.85, 123.75, 123.74, 61.13, 61.10, 55.6, 55.44, 55.41, 55.3, 43.7, 43.3, 32.3, 32.1, 27.69, 27.65, 24.7, 22.5; IR (ATR) ν_{max} 3273, 3062, 2932, 2861, 2818, 1650, 1592, 1537, 1475, 1433, 1371, 1246, 1149, 1126, 1048, 1001 cm^{-1}; LRMS (ESI) *m/z* 738 $[M + H]^+$; HRMS (ESI), m/z = 794.4454 $[M + H]^+$, 794.4460 calcd. for $C_{42}H_{56}N_{11}O_5^+$. Tetrapeptide **1** was complexed to zinc according to the above general procedure, affording **1·Zn_2** (tetranitrate salt) as a colourless solid in quantitative yield. ^{1}H NMR (500 MHz, MeOD) δ 8.68 (m, 4H), 8.15 (m, 4H), 7.69 (m, 8H), 4.40 (m, 4H), 4.13 (m, 6H), 3.80 (m, 4H), 2.64 (m, 4H), 1.91 (s, 3H), 1.51-1.91 (m, 8H), 1.21 (m, 4H); LRMS (ESI) *m/z* 307 $[M - 1H]^{3+}$; HRMS (ESI), m/z = 981.2694 $[M(NO_3) - 2H]^+$, 981.2686 calcd. for $C_{42}H_{53}N_{11}O_5Zn_2(NO_3)^+$.

Ac-Orn(DPA)-Gly-Orn(DPA)-Gly-NH_2 zinc complex, 2·Zn_2 Tetrapeptide **2** was synthesised on Rink amide resin (0.307 g, resin capacity 0.55 mmol g^{-1}), utilising the above general methods. Yield: 27.9 mg (22%); $[\alpha]_D^{20} = -17.3$ (*c* 0.50 MeOH); ^{1}H NMR (500 MHz, MeOD) δ 8.54 (m, 4H), 7.84 (m, 4H), 7.55 (m, 4H), 7.36 (m, 4H), 4.16-4.29 (m, 10H), 3.84 (m, 4H), 2.93 (m, 4H), 1.94 (s, 3H), 1.65-1.90 (m, 8H); ^{13}C NMR (125 MHz, MeOD) δ 175.1, 174.22, 174.15, 173.7, 172.0, 156.7, 155.8, 149.9, 149.8, 139.14, 139.09, 125.3, 125.2, 124.7, 124.6, 59.9, 59.6, 55.4, 55.1, 54.6, 43.8, 43.2, 29.9, 29.7, 23.1, 22.7, 22.5; IR (ATR) ν_{max} 3274, 3057, 2933, 2821, 1649, 1593, 1536, 1474, 1435, 1371, 1331, 1201, 1150, 1127, 1047, 998 cm^{-1}; LRMS (ESI) *m/z* 766 $[M + H]^+$; HRMS (ESI), *m/z* = 766.4143 $[M + H]^+$, 766.4147 calcd. for $C_{40}H_{52}N_{11}O_5^+$. Tetrapeptide **2** was complexed to zinc according to the above general procedure, affording **2·Zn_2** (tetranitrate salt) as a colourless solid in quantitative yield. ^{1}H NMR (400 MHz, MeOD)

δ 8.70 (m, 4H), 8.15 (m, 4H), 7.70 (m, 8H), 4.93 (m, 4H), 4.14 (m, 6H), 3.79 (m, 4H), 2.70 (m, 4H), 1.90 (s, 3H), 1.58-1.71 (m, 8H); LRMS (ESI) *m/z* 446 $[M - 2H]^{2+}$; HRMS (ESI), *m/z* = 955.2353 $[M(NO_3) - 2H]^+$, 955.2373 calcd. for $C_{40}H_{49}N_{11}O_5Zn_2(NO_3)^+$.

Ac-Dab(DPA)-Gly-Dab(DPA)-Gly-NH$_2$ zinc complex, 3·Zn$_2$ Tetrapeptide **3** was synthesised on Rink amide resin (0.455 g, resin capacity 0.55 mmol g^{-1}), utilising the above general methods. Yield: 48.5 mg (26%); $[\alpha]_D^{20} = -18.7$ (*c* 0.50 MeOH); ^{1}H NMR (500 MHz, MeOD) δ 8.43 (m, 4H), 7.73 (m, 4H), 7.51 (m, 4H), 7.24 (m, 4H), 4.45 (m, 1H), 4.41 (m, 1H), 3.71-3.85 (m, 12 H), 2.67 (m, 4H), 2.10 (m, 2H), 1.88-2.10 (m, 5H); ^{13}C NMR (100 MHz, MeOD) δ 175.4, 174.8, 174.4, 173.7, 172.1, 160.30, 160.27, 149.51, 149.48, 138.66, 138.66, 125.20, 125.18, 123.83, 123.82, 61.0, 53.7, 53.6, 52.2, 52.1, 43.8, 43.3, 29.9, 29.7, 22.6; IR (ATR) ν_{max} 3270, 3057, 2929, 2845, 1646, 1592, 1532, 1476, 1434, 1371, 1257, 1150, 1129, 1094, 1049, 1001 cm^{-1}; LRMS (ESI) *m/z* 738 $[M + H]^+$; HRMS (ESI), *m/z* = 738.3855 $[M + H]^+$, 738.3834 calcd. for $C_{38}H_{48}N_{11}O_5^+$. Tetrapeptide **3** was complexed to zinc according to the above general procedure, affording **3·Zn$_2$** (tetranitrate salt) as a colourless solid in quantitative yield. ^{1}H NMR (400 MHz, MeOD) δ 8.70 (m, 4H), 8.15 (m, 4H), 7.68 (m, 8H), 4.41 (m, 4H), 4.15 (m, 6H), 3.67-3.82 (m, 4H), 2.77 (m, 4H), 2.13 (m, 2H), 1.89-2.03 (m, 5H); LRMS (ESI) *m/z* 432 $[M - 2H]^{2+}$; HRMS (ESI), m/z = 925.2059 $[M(NO_3) - 2H]^+$, 925.2060 calcd. for $C_{38}H_{45}N_{11}O_5Zn_2(NO_3)^+$.

Ac-Dap(DPA)-Gly-Dap(DPA)-Gly-NH$_2$ zinc complex, 4·Zn$_2$ Tetrapeptide **4** was synthesised on Rink amide resin (0.313 g, resin capacity 0.55 mmol g^{-1}), utilising the above general methods. Yield: 28.4 mg (23%); $[\alpha]_D^{20} = -11.2$ (*c* 0.50 MeOH); ^{1}H NMR (500 MHz, MeOD) δ 8.46 (m, 4H), 7.74 (m, 4H), 7.45 (m, 4H), 7.26 (m, 4H), 4.53 (m, 1H), 4.48 (m, 1H), 3.75-4.01 (m, 12H), 3.05 (m, 2H), 2.96 (m, 2H), 1.95 (s, 3H); ^{13}C NMR (75 MHz, MeOD) δ 174.4, 173.9, 173.4, 171.9, 171.8, 159.8, 159.6, 149.6, 149.5, 138.8, 138.7, 125.2, 125.15, 123.93, 123.93, 61.0, 60.9, 57.3, 57.0, 53.9, 53.8, 43.8, 43.4, 22.7; IR (ATR) ν_{max} 3270, 3057, 2929, 2845, 1646, 1592, 1532, 1476, 1434, 1371, 1257, 1150, 1129, 1094, 1049, 1001 cm^{-1}; LRMS (ESI) *m/z* 710 $[M + H]^+$; HRMS (ESI), *m/z* = 710.3520 $[M + H]^+$, 710.3521 calcd. for $C_{36}H_{44}N_{11}O_5^+$. Tetrapeptide **4** was complexed to zinc according to the above general procedure, affording **4·Zn$_2$** (tetranitrate salt) as a colourless solid in quantitative yield. ^{1}H NMR (400 MHz, MeOD) δ 8.69 (m, 4H), 8.14 (m, 4H), 7.67 (m, 8H), 4.17-4.90 (m, 10H), 3.78-4.06 (m, 4H), 3.82-3.33 (m, 2H), 2.91 (m, 2H), 1.96 (s, 3H); LRMS (ESI) *m/z* 418 $[M - 2H]^{2+}$; HRMS (ESI), *m/z* = 417.5933 $[M - 2H]^{2+}$, 417.5932 calcd. for $C_{36}H_{41}N_{11}O_5Zn_2^{2+}$.

Ac-Dap(DPA)-Gly-Lys(DPA)-Gly-NH$_2$ Zinc complex, 5·Zn$_2$ Tetrapeptide **5** was synthesised on Rink amide resin (0.304 g, resin capacity 0.55 mmol g^{-1}), utilising the above general methods. Yield: 32.3 mg (26%); $[\alpha]_D^{20} = -22.3$ (*c* 0.50 MeOH); ^{1}H NMR (500 MHz, MeOD) δ 8.43 (m, 4H), 7.79 (m, 2H), 7.73 (m, 2H), 7.62 (m, 2H), 7.44 (m, 2H), 7.25 (m, 4H), 4.41 (m, 1H), 4.20 (m, 1H), 3.73-3.93 (m, 12 H), 3.00 (m, 1H), 2.91 (m, 1H), 2.51 (m, 2H), 1.98 (m, 3H), 1.78 (m, 1H), 1.63 (m, 1H), 1.54 (m, 2H), 1.33 (m, 2H); ^{13}C NMR (100 MHz, MeOD) δ 174.7, 174.4, 174.1, 173.5, 172.1, 160.7, 159.8, 149.7, 149.3, 138.8, 138.6, 125.1, 124.9, 123.9, 123.8, 61.1, 61.0, 57.0, 55.5, 55.4, 54.2, 43.8, 43.3, 32.1, 27.6, 24.7, 22.7; IR (ATR) ν_{max} 3275, 3059, 2931, 2859, 2825, 1645, 1592, 1568, 1531, 1475, 1433, 1371, 1248, 1149, 1127, 1094, 1048, 1001 cm^{-1}; LRMS (ESI) *m/z* 752 $[M + H]^+$; HRMS (ESI), *m/z* = 752.4019 $[M + H]^+$, 752.3991 calcd. for $C_{39}H_{50}N_{11}O_5^+$. Tetrapeptide **5** was complexed to zinc according to the above general procedure, affording **5·Zn$_2$** (tetranitrate salt) as a colourless solid in quantitative yield. ^{1}H NMR (400 MHz, MeOD) δ 8.70 (m, 4H), 8.17 (m, 4H), 7.69 (m, 8H), 4.52 (m, 4H), 4.38 (m, 2H), 4.10 (m, 4H), 3.77-3.97 (m, 4H), 3.21 (m, 1H), 2.92 (m, 1H), 2.67 (m, 2H), 1.94 (m, 3H), 1.51-1.69 (m, 4H), 1.19 (m, 2H); LRMS (ESI) *m/z* 439 $[M - 2H]^{2+}$; HRMS (ESI), m/z = 1002.2183 $[M(NO_3)_2 - H]^+$, 1002.2173 calcd. for $C_{39}H_{48}N_{11}O_5Zn_2(NO_3)_2^+$.

Anion binding studies

All measurements were performed in Krebs buffer or artificial urine[25] at pH 7.4 and at 25 °C.

General procedure for titrating the indicator PV with receptors 1–5·Zn$_2$. To a 1 cm quartz glass cuvette was added a solution of the indicator **PV** (2.5 mL, 20 μM) and to another matched quartz glass cuvette was added the buffer solution as the blank (2.5 mL). The absorbance spectrum was recorded from 250 – 750 nm. Aliquots of a solution containing the respective receptor (1000 μM) were then added to both the sample and the blank cuvettes. After each addition, the resulting solution was stirred for at least 30 seconds before the absorbance spectrum was recorded. Typically, up to 10 equiv. of the receptor were added to the solution. All titrations were repeated three times. To determine association constants for the receptor-indicator complexes, global analysis of the absorbance data over the range of 300 – 720 nm was carried out using a nonlinear least-squares curve fitting procedure, based on the equilibria described for 1 : 1 binding, using the commercially available software programme HypSpec® (Hyperquad® package).[23]

General procedure for titrating receptor-indicator ensembles with anions. Stock solutions of the respective 1 : 1 – receptor : **PV** ensemble (20 μM both) and of the tested phosphoanions as sodium salts (2000 μM) were prepared. To a 1 cm quartz glass cuvette was added a solution of the receptor-indicator ensemble (2.5 mL) and to another matched quartz glass cuvette was added a solution of the same concentration of the receptor as the blank (2.5 mL). The absorbance spectrum was recorded from 250 – 750 nm. Aliquots of the respective anion solution were then added to both the sample and the blank cuvettes. After each addition, the resulting solution was stirred for at least 30 seconds before the absorbance spectrum was recorded. Typically, up to 10 equivalents of the anion were added to the solution. All titrations were repeated three times. To determine association constants for the receptor-anion complexes, global analysis of the absorbance data over the range of 300 – 720 nm was carried out using a nonlinear least-squares curve fitting procedure, based on the equilibria described for indicator displacement,[24] using the com-

mercially available software program HypSpec® (Hyperquad® package).[23]

Acknowledgements

This research was funded by the Australian Research Council (DP140100227). VEZ thanks the DAAD for the award of a scholarship. The authors thank Karen K. Y. Yuen for assistance with the 2D NMR experiments and data analysis using Hyperquad®.

References

1 P. D. Beer and P. A. Gale, *Angew. Chem., Int. Ed.*, 2001, **40**, 486–516.
2 N. H. Evans and P. D. Beer, *Angew. Chem., Int. Ed.*, 2014, **53**, 11716–11754.
3 R. Martínez-Máñez and F. Sancenón, *Chem. rev.*, 2003, **103**, 4419–4476.
4 P. A. Gale, N. Busschaert, C. J. Haynes, L. E. Karagiannidis and I. L. Kirby, *Chem. Soc. Rev.*, 2014, **43**, 205–241.
5 S. Kubik, *Chem. Soc. Rev.*, 2010, **39**, 3648–3663.
6 S. Lee, K. K. Y. Yuen, K. A. Jolliffe and J. Yoon, *Chem. Soc. Rev.*, 2015, **44**, 1749–1762.
7 S. Xu, M. He, H. Yu, X. Cai, X. Tan, B. Lu and B. Shu, *Anal. Biochem.*, 2001, **299**, 188–193.
8 A. E. Timms, Y. Zhang, R. G. G. Russell and M. A. Brown, *Rheumatol.*, 2002, **41**, 725–729.
9 J. G. March, B. M. Simonet and F. Grases, *Clin. Chim. Acta*, 2001, **314**, 187–194.
10 D. H. Lee, S. Y. Kim and J.-I. Hong, *Angew. Chem., Int. Ed.*, 2004, **43**, 4777–4780.
11 H. K. Cho, D. H. Lee and J.-I. Hong, *Chem. Comm.*, 2005, 1690–1692.
12 H. N. Lee, Z. Xu, S. K. Kim, K. M. K. Swamy, Y. Kim, S.-J. Kim and J. Yoon, *J. Am. Chem. Soc.*, 2007, **129**, 3828–3829.
13 A. E. Hargrove, S. Nieto, T. Zhang, J. L. Sessler and E. V. Anslyn, *Chem. Rev.*, 2011, **111**, 6603–6782.
14 A. S. Rao, S. Singha, W. Choi and K. H. Ahn, *Org. Biomol. Chem.*, 2012, **10**, 8410–8417.
15 H. T. Ngo, X. Liu and K. A. Jolliffe, *Chem. Soc. Rev.*, 2012, **41**, 4928–4965.
16 K. Y. Yuen and K. A. Jolliffe, *Chem. Comm.*, 2013, **49**, 4824–4826.
17 X. Liu, H. T. Ngo, Z. Ge, S. J. Butler and K. A. Jolliffe, *Chem. Sci.*, 2013, **4**, 1680–1686.
18 V. J. Dungan, H. T. Ngo, P. G. Young and K. A. Jolliffe, *Chem. Comm.*, 2013, **49**, 264–266.
19 S. J. Butler and K. A. Jolliffe, *Chem. Asian J.*, 2012, **7**, 2621–2628.
20 M. S. Han and D. H. Kim, *Angew. Chem., Int. Ed.*, 2002, **114**, 3963–3965.
21 B. T. Nguyen and E. V. Anslyn, *Coord. Chem. Rev.*, 2006, **250**, 3118–3127.
22 Y. Zhou and J. Yoon, *Chem. Soc. Rev.*, 2012, **41**, 52–67.
23 P. Gans, A. Sabatini and A. Vacca, *Talanta*, 1996, **43**, 1739–1753.
24 K. A. Connors, *Binding constants: the measurement of molecular complex stability*, Wiley-Interscience, 1987.
25 T. Brooks and C. Keevil, *Lett. Appl. Microbiol.*, 1997, **24**, 203–206.
26 L. Zhang, G. S. Kauffman, J. A. Pesti and J. Yin, *J. Org. Chem.*, 1997, **62**, 6918–6920.
27 H. Kunz and C. Unverzagt, *Angew. Chem., Int. Ed.*, 1984, **23**, 436–437.